DALTON
FULL PAPER

Equilibrium and kinetic studies of (2,2′:6′,2″-terpyridine)gold(III) complexes. Preparation and crystal structure of $[Au(terpy)(OH)][ClO_4]_2$

Bruno Pitteri,*[a] Giampaolo Marangoni,[a] Fabiano Visentin,[a] Tatiana Bobbo,[a] Valerio Bertolasi[b] and Paola Gilli[b]

[a] *Dipartimento di Chimica, Università di Venezia, Calle Larga S. Marta 2137, 30123 Venezia, Italy*
[b] *Dipartimento di Chimica e Centro di Strutturistica Diffrattometrica, Università di Ferrara, Via Borsari 46, 44100 Ferrara, Italy*

Received 3rd August 1998, Accepted 23rd December 1998

Kinetic and equilibrium studies of the processes (1) and (2) (terpy = 2,2′:6′,2″-terpyridine) have been carried out in

$$[Au(terpy)Cl]^{2+} + H_2O \underset{k_{-1}}{\overset{k_1}{\rightleftharpoons}} [Au(terpy)(OH_2)]^{3+} + Cl^- \quad (1)$$

$$[Au(terpy)(OH_2)]^{3+} \overset{K_a}{\rightleftharpoons} [Au(terpy)(OH)]^{2+} + H^+ \quad (2)$$

water at 25 °C, $I = 0.1$ mol dm^{-3} ($LiClO_4$). Owing to the high charge of the metal centre, the $[Au(terpy)(OH_2)]^{3+}$ cation behaves as a strong acid ($K_a \geqslant 0.8$ mol dm^{-3}) and dissociates completely into the corresponding hydroxo species, which can be isolated in the solid state as its perchlorate. The crystal structure of $[Au(terpy)(OH)][ClO_4]_2$ has been determined by the single-crystal X-ray diffraction technique. It consists of *SP* (square planar) $[Au(terpy)(OH)]^{2+}$ cations having Au–N distances of 2.009(5), 2.008(4) and 1.949(4) Å and an Au–OH distance, the first experimentally determined, of 2.000(4) Å. The *SP* geometry is expanded to distorted tetragonal bipyramidal (*TBPY*) by linking the two perchlorate anions with Au–O distances of 3.023(8) and 3.069(8) Å, which are intermediate between bonding and van der Waals interactions. The secondary co-ordination phenomenon in gold(III) *SP* complexes is reviewed and a possible reason for its occurrence proposed.

Introduction

In the last few years there has been much interest in terpy complexes of platinum(II) and palladium(II) (terpy = 2,2′:6′,2″-terpyridine) in connection with the discovery that they show specific interactions with nucleic acids[1] as well as their intriguing spectroscopic and photophysical behaviour.[2] Besides, co-ordination compounds of the two metal ions have provided useful substrate for kinetic studies in substitution reactions at planar four-co-ordinate complexes. On the contrary, the chemistry of the related gold(III) complexes has remained undeveloped and the only species to have been reported are $[Au(terpy)Cl]Cl_2\cdot 3H_2O$ and the mixed-valence compound $[Au(terpy)Cl]_2[AuCl_2]_3[AuCl_4]$, both of which have been structurally characterized.[3] For the former a study of the product distribution in aqueous solution as a function of pH has also been reported. As a continuation of our studies on the synthesis and reactivity of d^8 transition-metal complexes containing the terpy ligand[4–7] we have isolated the complex $[Au(terpy)(OH)][ClO_4]_2$, the crystal structure of which is here reported, together with a kinetic and equilibrium study of the processes (1) and (2) in water, $I = 0.1$ mol dm^{-3} ($LiClO_4$), at 25 °C.

$$\underset{\mathbf{A}}{[Au(terpy)Cl]^{2+}} + H_2O \underset{k_{-1}}{\overset{k_1}{\rightleftharpoons}} \underset{\mathbf{B}}{[Au(terpy)(OH_2)]^{3+}} + Cl^- \quad (1)$$

$$\underset{\mathbf{B}}{[Au(terpy)(OH_2)]^{3+}} \overset{K_a}{\rightleftharpoons} \underset{\mathbf{C}}{[Au(terpy)(OH)]^{2+}} + H^+ \quad (2)$$

Experimental

Materials

The salt $KAuCl_4\cdot 2H_2O$ was prepared according to a standard procedure starting from metallic Au (99.99%). 2,2′:6′,2″-Terpyridine was obtained from Aldrich. Pure reagent grade LiCl, $LiClO_4$ and $AgClO_4$ (Fluka and Aldrich) were dried over P_2O_5 in a vacuum desiccator and used without further purification.

Instruments

Infrared spectra (4000–250 cm^{-1}, KBr discs and Nujol mulls; 400–150 cm^{-1}, polyethylene pellets) were recorded on a Nicolet Magna FT IR 750 spectrophotometer. Electronic spectra and kinetics measurements were obtained on a Perkin-Elmer Lambda 15 spectrophotometer. Proton NMR spectra were taken on a Bruker AC 200 F spectrometer. Conductivity measurements were carried out with a CDM 83 Radiometer Copenhagen conductivity meter and a CDC 334 immersion cell. Elemental analyses were performed by the Microanalytical Laboratory of the University of Padua.

Preparation of complexes

Chloro(2,2′:6′,2″-terpyridine)gold(III) chloride trihydrate, $[Au(terpy)Cl]Cl_2\cdot 3H_2O$. The preparation of this compound has been reported[3] but we used $KAuCl_4\cdot 2H_2O$ instead of $HAuCl_4\cdot 3H_2O$ as starting material.

Chloro(2,2′:6′,2″-terpyridine)gold(III) perchlorate, $[Au(terpy)Cl][ClO_4]_2$. The complex $[Au(terpy)Cl]Cl_2\cdot 3H_2O$ (0.591 g, 1 mmol) was dissolved in hot water (40 cm^3). After addition of an excess of solid $LiClO_4$, slow cooling of the solution at room temperature resulted in the formation of the ochre crystalline product, which was filtered off, washed with cold water (2–3 cm^3) and dried *in vacuo*. Yield > 90% (Found: C, 27.2; H, 1.50;

Cl, 16.1; N, 6.32. $C_{15}H_{11}AuCl_3N_3O_8$ requires C, 27.1; H, 1.67; Cl, 16.0; N, 6.32%). Λ_M (dmf = dimethylformamide) = 179 Ω^{-1} cm^2 mol^{-1}. IR: $\tilde{\nu}$ (Au–Cl) = 353 cm^{-1} (polyethylene pellets).

Hydroxo(2,2′:6′,2″-terpyridine)gold(III) perchlorate, [Au(terpy)(OH)][ClO$_4$]$_2$. Silver perchlorate (0.207 g, 1 mmol) was added to a hot aqueous solution (50 cm^3) of [Au(terpy)Cl][ClO$_4$]$_2$ (0.665 g, 1 mmol) and the mixture stirred in the dark for 30 min. The AgCl formed was filtered off and the warm solution treated with an excess of solid $LiClO_4$. On slow cooling of the solution at room temperature, well formed beige crystals were separated, then filtered off, washed with the minimum amount of cold water and dried *in vacuo*. Yield ≈ 80% (Found: C, 27.8; H, 1.62; Cl, 11.2; N, 6.42. $C_{15}H_{12}AuCl_2N_3O_9$ requires C, 27.9; H, 1.87; Cl, 11.0; N, 6.50%). Λ_M (dmf) = 160 Ω^{-1} cm^2 mol^{-1}. IR: $\tilde{\nu}$ (O–H) = 3425 cm^{-1} (Nujol mulls).

Kinetics

The forward process was followed spectrophotometrically by measuring the changing absorbance at a suitable wavelength (366 nm) as a function of time and initiated by adding 2–20 μl of a 0.015 mol dm^{-3} dmf solution of the substrate complex, [Au(terpy)Cl][ClO$_4$]$_2$, to 3 cm^3 of an aqueous solution of 0.1 mol dm^{-3} $LiClO_4$ previously brought to the reaction temperature (25 °C) in a thermostatted cell in the spectrophotometer. The reverse process was followed starting from a 1×10^{-5} mol dm^{-3} aqueous solution of [Au(terpy)(OH)][ClO$_4$]$_2$ with an excess of chloride, in order to provide pseudo-first-order conditions, in the presence of added acid ($HClO_4$). Pseudo-first-order rate constants (k_{obs}/s^{-1}) were obtained either from the gradients of plots of $\log(D_t - D_\infty)$ *vs.* time or from a non linear least-squares fit of experimental data from the equation $D_t = D_\infty + (D_o - D_\infty)\exp(-k_{obs}t)$, where D_o, D_∞ and k_{obs} are the parameters to be optimized (D_o = absorbance after mixing of reactants, D_∞ = absorbance at completion of reaction). Errors on individual k_{obs} determinations are in the ±5% range.[8]

^{1}H NMR experiments

Experimental conditions: solvent D_2O, solvent peak at δ 4.65 *vs.* Me_4Si as reference, 25 °C. (a) 0.035 mol dm^{-3} [Au(terpy)Cl]$Cl_2 \cdot 3H_2O$: δ 9.17 (2 H, d, J = 6 Hz; H_a), 8.70 (7 H, m, $H_{c,d,e,f}$) and 8.04 (2 H, m, H_b). (b) 0.017 mol dm^{-3} [Au(terpy)Cl]$Cl_2 \cdot 3H_2O$ and 0.1 mol dm^{-3} Cl^-: δ 9.17 (2 H, d, J = 6 Hz, H_a), 8.70 (7 H, m, $H_{c,d,e,f}$) and 8.04 (2 H, m, H_b). (c) 0.004 mol dm^{-3} [Au(terpy)(OH)][ClO$_4$]$_2$: δ 8.82 (2 H, d, J = 5.8 Hz; H_a), 8.61 (7 H, m, $H_{c,d,e,f}$) and 8.03 (2 H, m, H_b). (d) 0.002 mol dm^{-3} [Au(terpy)(OH)][ClO$_4$]$_2$ and 0.1 mol dm^{-3} Cl^-: δ 8.82 (2 H, d, J = 5.8 Hz; H_a), 8.61 (7 H, m, $H_{c,d,e,f}$) and 8.03 (2 H, m, H_b). (e) 0.002 mol dm^{-3} [Au(terpy)Cl][ClO$_4$]$_2$: signals of both [Au(terpy)Cl]$^{2+}$ and [Au(terpy)(OH)]$^{2+}$ cations in ≈2 : 1 ratio.

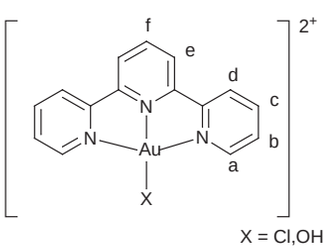

Crystallography

X-Ray intensities were collected at room temperature on an Enraf-Nonius CAD4 diffractometer using graphite monochromated Mo-Kα radiation (λ = 0.71069 Å) with the ω–2θ scan technique. Lattice constants were determined by least-squares fitting of the setting angles of 25 reflections in the range $9 \leqslant \theta \leqslant 14°$. Intensities of three standard reflections were measured every 2 h and did not show significant variations. All intensities were corrected for Lorentz-polarization and absorption effects (ψ-scan method, minimum transmission factor 0.37). The structure was solved by Patterson and Fourier methods. All hydrogen atoms were localized in the difference synthesis computed after the first refinement cycles. Final full-matrix least-squares refinement was carried out with anisotropic non-hydrogen atoms and isotropic hydrogens, except for the hydrogen bonded to the O(1) atom which, for instability problems during the refinement, was fixed at the position located in the Fourier-difference map. However, the hydrogen positions are not completely reliable and in particular that of the hydrogen bonded to O(1) has to be considered highly problematic as far as X-ray diffraction is concerned. The final difference map showed a peak of 1.47 e $Å^{-3}$ at 0.92 Å from the Au atom and no other peaks greater than 0.43 e $Å^{-3}$ outside the co-ordination sphere. The programs used and sources of scattering factor data are given in ref. 9.

CCDC reference number 186/1296.

See http://www.rsc.org/suppdata/dt/1999/677/ for crystallographic files in .cif format.

Results and discussion

Solution chemistry of (2,2′:6′,2″-terpyridine)gold(III) complexes

When complex **A** is dissolved as its perchlorate salt in water (25 °C, I = 0.1 mol dm^{-3}, $LiClO_4$) in the concentration range 2×10^{-5}–10^{-4} mol dm^{-3} the spectrophotometric changes observed in repetitive scanning of the solution spectrum are characteristic of a single kinetically detectable stage, with well maintained isosbestic points at 341, 352 and 358 nm. Careful examination of the spectral changes and the close similarity of the spectra at the end of reaction to those of authentic samples of **C** at the same concentration as the starting **A** demonstrate that, according to the usual associatively activated mechanism for substitution reactions at d^8 square planar *SP* complexes,[10] the direct process that has been studied kinetically involves the displacement of co-ordinated chloride by H_2O with formation of **B**, which dissociates rapidly and completely giving the corresponding hydroxo species **C**. The latter, isolated as its perchlorate, is a non-reactive species. Dissolved either in water or in aqueous chloride solutions in the 0.05–1 mol dm^{-3} range of concentrations, its UV/VIS spectrum does not change even after a long time. This finding is confirmed by ^{1}H NMR spectra [Experimental section, experiments (c), (d)]. The reverse process could then be studied only with an excess of chloride in the presence of added acid ($HClO_4$) which allows the hydroxo species **C** to be partially converted into the corresponding reactive aqua-complex **B** by a rapid proton transfer reaction. Under these conditions, the rate law of the overall process, derived by a combination of the kinetic law for the disappearance of **A** ($-d[\mathbf{A}]/dt = k_1[\mathbf{A}] - k_{-1}[\mathbf{B}][Cl^-]$) with the mass balance ($C_0 = [\mathbf{A}] + [\mathbf{B}] + [\mathbf{C}]$) and the equilibrium constant ($K_a = [H^+][C]/[B]$), can be expressed as in eqn. (3) (where k_1 is

$$k_{obs} = k_1 + (k_{-1}[Cl^-][H^+])/(K_a + [H^+]) \qquad (3)$$

the solvolytic rate constant for the replacement of Cl^- by water, k_{-1} the second-order rate constant for the reverse reaction, and K_a the acidity constant for deprotonation of the co-ordinated H_2O in **B**). For the direct process, in absence of any reagents added, eqn. (3) reduces to $k_{obs} = k_1$, which can be directly determined from the absorbance change *vs.* time at a convenient wavelength (366 nm); k_1 values obtained starting from different concentrations of **A** are reported in Table 1.

As far as the reverse process is concerned, the first-order rate constants, k_{obs}, at different [H^+] and [Cl^-] values are listed in Table 2. Plots of k_{obs} against [Cl^-] at different [H^+] concentrations give straight lines for each set of experiments with slopes $k_{-1}[H^+]/(K_a + [H^+])$ and finite intercepts, k_1 (Table 3), the

Table 1 First-order rate constants, $k_{obs} = k_1$, for the reaction $[Au(terpy)Cl]^{2+} + H_2O \rightleftharpoons [Au(terpy)(OH_2)]^{3+} + Cl^-$ in water at 25 °C [I = 0.1 mol dm^{-3} ($LiClO_4$)]

10^3[Au(terpy)Cl]$^{2+}$/mol dm^{-3}	k_1/s^{-1}
0.025	0.0178 ± 0.0005
0.050	0.0173 ± 0.0005
0.100	0.0179 ± 0.0004

Table 2 First-order rate constants, k_{obs}, for the overall reverse process in water at 25 °C [I = 0.1 mol dm^{-3} ($LiClO_4$, $HClO_4$)] [a]

[H$^+$]/mol dm^{-3}	10^3[Cl$^-$]/mol dm^{-3}	$10^2 k_{obs}$/s^{-1}
0.003	0.097	2.00
	0.194	2.62
	0.291	3.12
	0.388	3.72
	0.485	4.42
0.007	0.097	3.00
	0.194	4.56
	0.291	6.11
	0.388	9.00
0.010	0.090	3.73
	0.180	5.50
	0.225	6.50
	0.270	7.50
	0.315	8.10
	0.450	11.8
0.020	0.1	5.6
	0.2	9.4
	0.3	13.8
	0.4	16.6
0.030	0.1	7.7
	0.2	13.8
	0.3	19.5
	0.4	26.1
0.040	0.10	8.0
	0.14	11.4
	0.20	14.9
	0.26	18.3
0.060	0.10	12.6
	0.20	23.7
	0.30	34.2
0.080	0.10	16.9
	0.14	25.8
	0.20	31.2
	0.26	39.2

[a] Errors on individual k_{obs} determinations are in the range ± 5% (ref. 8). Substrate concentration: 1×10^{-5} mol dm^{-3}.

Table 3 First-order rate constants, k_1, and $k_{-1}[H^+]/(K_a + [H^+])$ values for the overall reverse process in water at 25 °C and different [H$^+$] [I = 0.1 mol dm^{-3} ($LiClO_4$, $HClO_4$)]

[H$^+$]/mol dm^{-3}	k_1 [a]/s^{-1}	$k_{-1}[H^+](K_a + [H^+])^{-1}$ [a]/dm^3 mol^{-1} s^{-1}
0.003	0.0139 ± 0.0006	61 ± 2
0.007	0.008 ± 0.006	200 ± 20
0.010	0.015 ± 0.003	220 ± 10
0.020	0.020 ± 0.006	370 ± 20
0.030	0.016 ± 0.003	610 ± 10
0.040	0.021 ± 0.007	630 ± 40
0.060	0.019 ± 0.004	1080 ± 20
0.080	0.032 ± 0.003	1390 ± 20

[a] Determined starting from [Au(terpy)(OH)]$^{2+}$ as intercepts and slopes of straight lines obtained from plots of k_{obs} against [Cl$^-$] at different [H$^+$] concentrations using the values listed in Table 2.

mean of which (0.018 s^{-1}) is in close agreement with the k_1 obtained, with larger accuracy, starting from **A** (Table 1). As a plot of the slopes against [H$^+$] is linear over the whole examined acidity range (0.003–0.08 mol dm^{-3}) (Fig. 1), K_a must be at least ten times greater than the highest [H$^+$], *i.e.* $K_a \geqslant 0.8$ mol dm^{-3},

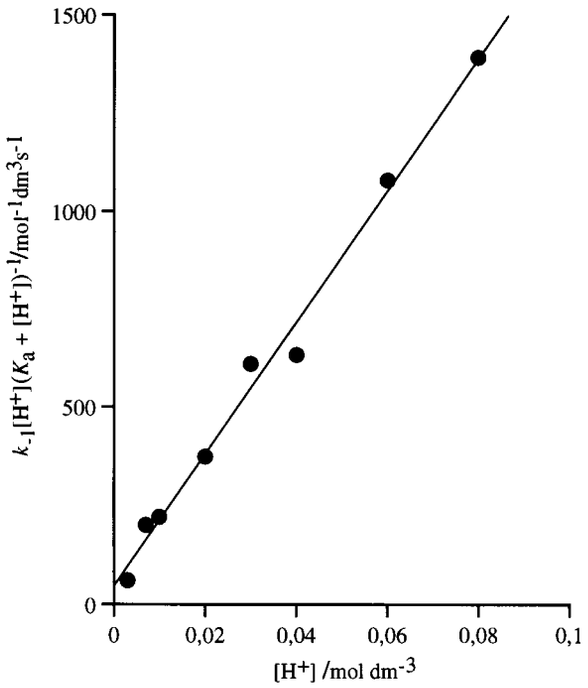

Fig. 1 Plot of the $k_{-1}[H^+]/(K_a + [H^+])$ slopes against [H$^+$] (Table 3).

which leads to the conclusion that **B** behaves as a strong acid in accordance with the high positive charge on the complex. Under these experimental conditions, eqn. (3) can be thus simplified into eqn. (4), which allows one to calculate a series of

$$k_{obs} = k_1 + (k_{-1}[Cl^-][H^+]/K_a) \quad (4)$$

k_{-1}/K_a values by dividing the terms $k_{-1}[H^+]/K_a$ by experimental [H$^+$]. From the mean (20000 ± 3000 dm^6 mol^{-2} s^{-1}) the k_{-1} rate constant relative to the replacement of co-ordinated water by chloride can therefore be estimated as ⩾16000 dm^3 mol^{-1} s^{-1}. Consequently, k_1/k_{-1}, *i.e.* the equilibrium constant, K_{H_2O}, for the reaction $\mathbf{A} + H_2O \rightleftharpoons \mathbf{B} + Cl^-$, is ⩽1.1 × 10^{-6} mol dm^{-3} and the overall equilibrium constant of the system, as expressed by eqn. (5), is ≈8.8 × 10^{-7} mol^2 dm^{-6}, also in accordance with

$$K_{H_2O}K_a = [\mathbf{C}][Cl^-][H^+]/[\mathbf{A}] \quad (5)$$

the results of the ^{1}H NMR experiments (a)–(e). In particular, under the conditions used in experiments (a), (b), both the spectra correspond to the spectrum of pure [Au(terpy)Cl]$^{2+}$.[3] Furthermore, the spectrum of pure [Au(terpy)(OH)]$^{2+}$ [experiment (c)] does not change in the presence of 0.1 mol dm^{-3} Cl$^-$ [experiment (d)]. Finally [experiment (e)], the spectrum of a 0.002 mol dm^{-3} [Au(terpy)Cl]$^{2+}$ solution exhibits resonances of both [Au(terpy)Cl]$^{2+}$ and [Au(terpy)(OH)]$^{2+}$ in ≈2 : 1 ratio.

Structure of [Au(terpy)(OH)][ClO$_4$]$_2$

Crystal data, data collection and refinement details are given in Table 4 and selected bond distances and angles are given in Table 5.

An ORTEP[11] view of the complex together with its two perchlorate counter anions is shown in Fig. 2. The four positions of the square-planar (*SP*) co-ordination of the Au^{III} are occupied by the three nitrogens of the terpy ligand and a further hydroxide group. The ligand is approximately planar, the maximum displacement, Δ, of a non-hydrogen atom from the mean plane being 0.071 Å. The Au atom lies on this plane (Δ = 0.046 Å) and the O(1) atom of the hydroxide group is slightly out of it by 0.146 Å.

The co-ordination geometry of the gold atom is considerably distorted from the perfect *SP* geometry, the two N–Au–N

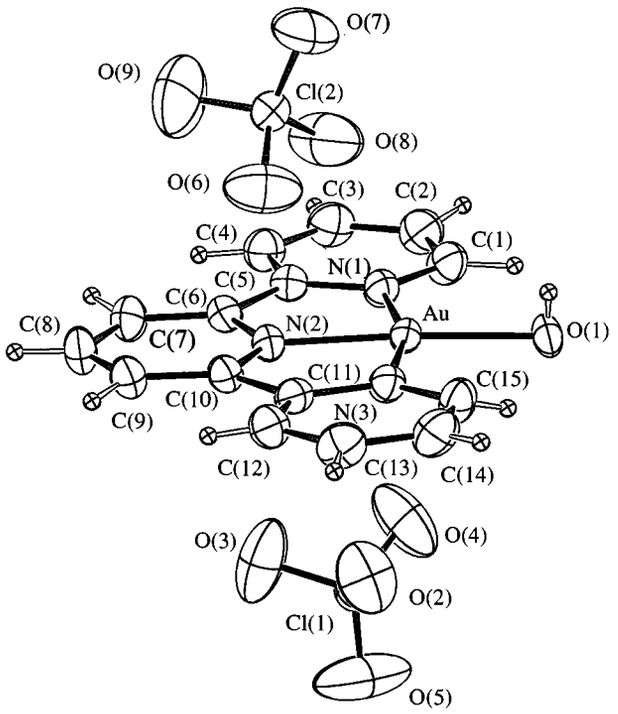

Fig. 2 An ORTEP[11] view of $[Au(terpy)(OH)][ClO_4]_2$ showing thermal ellipsoids at 30% probability and the atom numbering scheme.

angles being 81.2(2) and 81.5(2)° and the N–Au–O ones 100.0(2) and 97.4(2)°. Not even the three Au–N distances are equivalent, the two opposite Au–N(1) and Au–N(3) bonds having rather similar lengths, 2.009(5) and 2.008(4) Å, at variance with the Au–N(2) which is rather shorter (1.949(4) Å). This pattern of distances and angles seems to be typical of all known *SP* Au(terpy) complexes listed in Table 6, which illustrate another interesting effect, *i.e.* the intercorrelation between the Au–N distance and the C–N–C internal angle of the pyridine donor. The shorter Au–N(2) bond [on average 1.940(7) Å] is associated with a wider C–N–C angle of 124.4(8)°, while the longer Au–N(1) and Au–N(3) bonds [on average 2.019(9) Å] meet with a narrower angle of 121.0(5)°. This trend, that is clearly interpretable within the frame of the VSEPR theory[12] as well as by Bent's rule,[13] is confirmed by a number of different measurements of this angle, such as: (*a*) 116.94(3)° in the microwave structure of free pyridine;[14] (*b*) 117(1)° in the crystal structure of the free terpy ligand;[15] (*c*) 121(1)° in a number of *SP* gold(III) complexes co-ordinating the "free" pyridine ligand at an average Au^{III}–N distance of 2.03(1) Å; and finally, (*d*) 124.4(8)° in the three $[Au(terpy)X]^{2+}$ complexes of Table 6 as far as the "compressed" Au–N(2) bond is concerned.

The Au–OH distance of 2.000(4) Å cannot be compared with that of any other gold(III) structure having the same type of bond but only with the Au^{III}–O in carboxylates which is in the range of 2.00–2.07 Å.[16]

Figs. 2 and 3 show that the *SP* complex is able to expand the co-ordination geometry to distorted *TBPY* (tetragonal bipyramidal) by forming secondary Au–O bonds with the oxygens of the perchlorate anions having distances of 3.023(8) and 3.069(8) Å, longer than normal Au-O bonds but much shorter than the usual non-bonded contacts between these atoms (some 3.6 Å).[17] In the present case, two of such distorted *TBPY*s associate in dimers through two O–H···O^- hydrogen bonds [d(O···O) = 2.798(9) Å] linking the co-ordinated OH groups to the perchlorate anions.

Such a secondary co-ordination of anions is, by itself, interesting because secondary bonding phenomena are known to be possible indicators of incipient chemical reactions since the seminal papers published by Bent (1968) and Alcock (1972).[18] A preliminary study[19] has shown that secondary co-ordination

Table 4 Crystal data and details of data collection and refinement procedure for $[Au(terpy)(OH)][ClO_4]_2$

Formula	$[AuC_{15}H_{12}ON_3]^{2+}2[ClO_4]$
M	646.15
Space group	$P\bar{1}$ (no. 2)
Crystal system	Triclinic
a/Å	9.006(1)
b/Å	12.361(4)
c/Å	8.790(2)
α/°	99.13(2)
β/°	102.86(2)
γ/°	82.93(2)
U/Å^3	938.0(4)
Z	2
D_c/g cm^{-3}	2.288
$F(000)$	616
μ(Mo-Kα)/cm^{-1}	81.85
Crystal size/mm	0.10 × 0.26 × 0.50
Measured reflections	4822
Independent reflections	4532
R_{int}	0.027
Observed reflections (N_o)	3882 [$I > 3\sigma(I)$]
$\theta_{min} - \theta_{max}$/°	2–28
hkl ranges	−11, 11; −16, 16; 0, 11
R	0.032
R'	0.041
No. variables (N_v)	315
Goodness of fit	1.301

Table 5 Selected distances (Å) and angles (°) for $[Au(terpy)(OH)][ClO_4]_2$

Au–N(1)	2.009(5)	N(1)–C(1)	1.351(7)
Au–N(2)	1.949(4)	N(1)–C(5)	1.359(9)
Au–N(3)	2.008(4)	N(2)–C(6)	1.354(8)
Au–O(1)	2.000(4)	N(2)–C(10)	1.345(6)
Au···O(4)	3.069(8)	N(3)–C(11)	1.351(8)
Au···O(8)	3.023(8)	N(3)–C(15)	1.346(9)
		C(5)–C(6)	1.463(7)
O(1)···O(7)	2.798(9)	C(10)–C(11)	1.489(9)
N(1)–Au–N(2)	81.2(2)	O(4)–Au–O(8)	151.0(5)
N(2)–Au–N(3)	81.5(2)	Au–N(1)–C(1)	125.4(4)
N(1)–Au–N(3)	162.6(2)	Au–N(1)–C(5)	113.2(4)
N(1)–Au–O(1)	100.0(2)	C(1)–N(1)–C(5)	121.4(5)
N(2)–Au–O(1)	176.9(2)	Au–N(2)–C(6)	117.2(3)
N(3)–Au–O(1)	97.4(2)	Au–N(2)–C(10)	117.4(3)
N(1)–Au–O(4)	79.8(4)	C(6)–N(2)–C(10)	125.4(4)
N(2)–Au–O(4)	87.1(4)	Au–N(3)–C(11)	113.3(4)
N(3)–Au–O(4)	100.4(4)	Au–N(3)–C(15)	126.0(4)
O(1)–Au–O(4)	90.3(5)	C(11)–N(3)–C(15)	120.7(5)
N(1)–Au–O(8)	78.0(5)	N(1)–C(5)–C(6)	115.8(5)
N(2)–Au–O(8)	71.2(4)	N(2)–C(6)–C(5)	112.7(5)
N(3)–Au–O(8)	95.3(4)	N(2)–C(10)–C(11)	112.3(4)
O(1)–Au–O(8)	111.7(5)	N(3)–C(11)–C(10)	115.6(5)

of anions is common in gold(III) *SP* complexes and gives rise to isolated tetragonal pyramids (*TPY*) and bipyramids (*TBPY*), as well as to μ_2-anion *TPY* dimers or infinite *TBPY* chains. Systematic investigation of the CSD (Cambridge Structural Database)[20] shows that this geometry expansion is largely prevalent for gold(III) *SP* complexes but is seldom shared by the corresponding compounds of Pt^{II} and Pd^{II} which prefer to form dimers (or sometimes) chains involving metal–metal interactions. Table 7 reviews, as typical examples, all cases of charged *SP* gold(III) complexes with nitrogen ligands and *TPY* or *TBPY* secondary co-ordination retrievable from CSD. Secondary ligands are, in increasing order of average contact distance, H_2O [3.03(1)], ClO_4^- [3.10(9)], Cl^- [3.13(6)], BF_4^- [3.19(2)], NO_3^- [3.21(6)], Br^- [3.24(5)] and $AuCl_4^-$ [3.52(1) Å], that, with the possible exception of the $AuCl_4^-$ anions, are far shorter than van der Waals contact distances (*e.g.* 4.0 for Au–Cl and 3.6 Å for Au–O).[19]

This secondary co-ordination in a *SP* complex of a d^8 metal ion, such as Au^{III}, cannot be interpreted as a co-ordination

Table 6 Comparison of the geometries (distances in Å, angles in °) for some $[Au(terpy)X]^{2+}$ *SP* complexes (nitrogen labels as in Fig. 2)

Complex	Au–N(1) Au–N(3)	Au–N(2)	C–N(1)–C C–N(3)–C	C–N(2)–C	N(1)–Au–N(2) N(3)–Au–N(2)	Ref.
$[Au(terpy)Cl]Cl_2 \cdot 3H_2O$	2.018(6)	1.931(7)	121.1(7)	123.4(7)	81.4(3)	3
	2.029(6)		121.5(7)		81.4(3)	
$[Au(terpy)Cl]_2[AuCl_2]_3[AuCl_4]$	2.022(9)	1.941(8)	121.0(9)	124.5(9)	81.3(4)	3
	2.030(8)		120.1(9)		81.4(4)	
$[Au(terpy)(OH)][ClO_4]_2$	2.009(5)	1.949(4)	121.4(5)	125.4(4)	81.2(2)	This work
	2.008(4)		120.7(5)		81.5(2)	
Average	2.019(9)	1.940(7)	121.0(5)	124.4(8)	81.4(1)	

Table 7 Pseudo-octahedral secondary co-ordination in gold(III) square-planar complexes (distances in Å and e.s.d.s of the averages in square brackets)

Refcode	Complex	X	Ligand	Motif	*d*(Au–X)/Å
This work	$[Au(terpy)(OH)]^{2+}$	O	ClO_4^-	*TBPY*	3.023(8)/3.069(8)
CAEAUC	$[Au(dien)Cl]^{2+}$	O	ClO_4^-	Chain	3.089/3.103
AEMAUP	$[Au(dien)Cl]^{2+}$	O	ClO_4^-	*TBPY*	3.102
ZELCAU	$[Au(pmpterpy)Cl]^{2+}$	O	ClO_4^-	*TBPY*	2.899/3.192
POPKUA	$[Au(tacyd)]^{3+}$	O	ClO_4^-	*TBPY*	3.194/3.250
POPKUA	$[Au(tacyd)]^{3+}$	O	ClO_4^-	*TBPY*	3.035
	Average	O	ClO_4^-		⟨3.10[9]⟩
POPKUA	$[Au(tacyd)]^{3+}$	O	NO_3^-	*TBPY*	3.150/3.263
	Average	O	NO_3^-		⟨3.21[6]⟩
BUYMOX	$[Au(terpy)Cl]^{2+}$	O	H_2O	*TBPY*	3.022
BENYEY	$[Au(py)_2Cl_2]^+$	O	H_2O	*TBPY*	3.045
	Average	O	H_2O		⟨3.03[1]⟩
ZENFED	$[Au(bipy)Cl_2]^+$	F	BF_4^-	Chain	3.165/3.213
	Average	F	BF_4^-		⟨3.19[2]⟩
DODXID	$[Au(dien)Cl]^{2+}$	Cl	Cl^-	*TBPY*	3.121/3.183
TEMMED	$[Au(hacytd)]^{3+}$	Cl	Cl^-	*TBPY*	3.096/3.096
JIHGOW	$[Au(en)_2]^{3+}$	Cl	Cl^-	*TBPY*	3.101/3.101
AEMAUP	$[Au(dien)Cl]^{2+}$	Cl	Cl^-	*TBPY*	3.05
BUYMOX	$[Au(terpy)Cl]^{2+}$	Cl	Cl^-	*TBPY*	3.049
BENYEY	$[Au(py)_2Cl_2]^+$	Cl	Cl^-	*TBPY*	3.171
VEGMEZ	$[Au(bipy)Cl_2]^+$	Cl	Cl^-	μ_2-Cl	3.211/3.224
	Average	Cl	Cl^-		⟨3.13[6]⟩
FUJFEV	$[Au(tpp)]^+$	Cl	$AuCl_4^-$	Chain	3.521/3.521
VIWKOB	$[Au(tdacyn)Cl_2]^+$	Cl	$AuCl_4^-$	*TPY*	3.525
	Average	Cl	$AuCl_4^-$		⟨3.522[2]⟩
FUHLOJ	$[Au(phen)(CN)_2]^+$	Br	Br^-	Chain	3.277/3.277
FUHLUP	$[Au(phen)(CN)_2]^+$	Br	Br^-	μ_2-Br	3.165/3.165
	Average	Br	Br^-		⟨3.24[5]⟩

terpy = 2,2′ : 6′,2″-Terpyridine; dien = diethylenetriamine; pmpterpy = 4′-(*p*-methoxyphenyl)-2,2′ : 6′,2″-terpyridine; tacyd = 1,4,8,11-tetraazacyclotetradecane; py = pyridine; bipy = 2,2′-bipyridine; hacytd = 1,8-bis(2-hydroxyethyl)-1,3,6,8,10,13-hexaazacyclotetradecane; en = ethylenediamine; tpp = 5,10,15,20-tetraphenylporphyrinate; tdacyn = 1-thia-4,7-diazacyclononane. *TBPY* = Isolated tetragonal bipyramid; chain = *TBPY* chain; μ_2 = *TPY* (tetragonal pyramid) dimer.

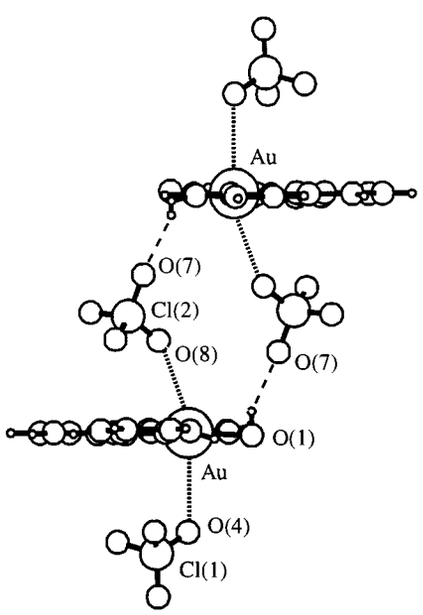

Fig. 3 The observed packing motif where two *TBPY* $[Au(terpy)(OH)][ClO_4]_2$ dimerize by O–H · · · $^-$O hydrogen bond formation.

expansion because of the great stability of the *SP* geometry for metal ions of such a configuration having large values of 10 *Dq*, which is the case of Au^{III} owing to both its position in the third transition series and its high oxidation number. The interaction is thus to be considered as an electrostatic perturbation of the essentially stable d^8 low-spin square-planar complex. Rather paradoxically, such a perturbation is allowed to become the stronger (and the additional bond the shorter) the higher is the 10*Dq*, because the axial perturbation splits the non-bonding $d(z^2)$ metal orbital and the *SP* complex can remain stable only when the doubly filled $d(z^2)^*$ molecular orbital so generated is lower in energy than the empty antibonding $d(x^2 - y^2)^*$ one. This may help to understand why secondary co-ordination in d^8 *SP* complexes is mostly observed for gold(III) compounds.

Acknowledgements

We thank the Italian Ministry of University and Scientific Research for financial support.

References

1 E. C. Constable, *Adv. Inorg.Chem. Radiochem.*, 1986, **30**, 69.
2 H.-K. Yip, L.-K. Cheng, K.-K. Cheung and C.-M. Che, *J. Chem. Soc.*, *Dalton Trans.*, 1993, 2933 and refs. therein.

3 L. S. Hollis and S. J. Lippard, *J. Am. Chem. Soc.*, 1983, **105**, 4293.
4 G. Marangoni, B. Pitteri, G. Chessa, V. Ferretti, P. Gilli and V. Bertolasi, *Acta Crystallogr.*, *Sect. C*, 1992, **48**, 814.
5 B. Pitteri, G. Marangoni, L. Cattalini and T. Bobbo, *J. Chem. Soc.*, *Dalton Trans.*, 1995, 3853.
6 G. Annibale, M. Brandolisio and B. Pitteri, *Polyedron*, 1995, **14**, 451.
7 B. Pitteri, G. Marangoni, F. Visentin, L. Cattalini and T. Bobbo, *Polyedron*, 1998, **17**, 475.
8 L. Canovese, L. Cattalini, P. Uguagliati and L. M. Tobe, *J. Chem. Soc.*, *Dalton Trans.*, 1990, 867.
9 MOLEN, An Interactive Structure Solution Procedure, Enraf-Nonius, Delft, 1990; PARST 96, M. Nardelli, *J. Appl. Crystallogr.*, 1995, **28**, 659; M. Nardelli, PARSTCIF, Program for Creating a CIF from the Output of PARST, University of Parma, 1991; D. T. Cromer and J. T. Waber, *International Tables for X-Ray Crystallography*, Kynoch Press, Birmingham, 1974.
10 F. Basolo and R. G. Pearson, *Mechanism of Inorganic Reactions*, 2nd edn., Wiley, New York, 1967, pp. 410–414.
11 C. K. Johnson, ORTEP II, Report ORNL-5138, Oak Ridge National Laboratory, Oak Ridge, TN, 1976.
12 R. J. Gillespie, *Molecular Geometry*, Van Nostrand-Reinhold, London, 1972; *J. Chem. Educ.*, 1963, **40**, 295; 1970, **47**, 18.
13 H. A. Bent, *J. Chem. Educ.*, 1960, **37**, 616; *Chem. Rev.*, 1961, **61**, 275.
14 Landolt-Börnstein, *Numerical Data and Functional Relationships in Science and Technology*, *New Series*, ed. K.-H. Hellwege and A. H. Hellwege; vol. 7, *Structure Data of Free Polyatomic Molecules*, Springer, Berlin, 1976.
15 C. A. Bessel, R. F. See, D. L. Jameson, M. R. Churchill and K. J. Takauchi, *J. Chem. Soc.*, *Dalton Trans.*, 1992, 3233.
16 A. Dar, K. Moss, S. M. Cottrill, R. V. Parish, C. A. McAuliffe, R. G. Pritchard, B. Beagley and J. Sandbank, *J. Chem. Soc.*, *Dalton Trans.*, 1992, 1907; A. G. Orpen, L. Brammer, F. H. Allen, O. Kennard, D. G. Watson and R. Taylor, *J. Chem. Soc.*, *Dalton Trans.*, 1989, S1.
17 G. Nardin, L. Randaccio, G. Annibale, G. Natile and B. Pitteri, *J. Chem. Soc.*, *Dalton Trans.*, 1980, 220.
18 H. A. Bent, *Chem. Rev.*, 1968, **68**, 587; N. W. Alcock, *Adv. Inorg. Chem. Radiochem.*, 1972, **15**, 1.
19 G. Marangoni, B. Pitteri, V. Bertolasi, V. Ferretti and G. Gilli, *J. Chem. Soc.*, *Dalton Trans.*, 1987, 2235.
20 F. H. Allen, S. Bellard, M. D. Brice, B. A. Cartwright, A. Doubleday, H. Higgs, B. G. Hummelink-Peters, O. Kennard, W. D. S. Motherwell, J. R. Rogers and D. G. Watson, *Acta Crystallogr.*, *Sect. B*, 1979, **35**, 2331; F. H. Allen and O. Kennard, *Chem. Des. Autom. News*, 1993, **8**, 1, 31–37.

Paper 8/06098C